16

Environment-Induced Silk Fibroin Conformation Based on the Magnetic Resonance Spectroscopy

Teng Jiang and Ping Zhou
The Key laboratory of Molecular Engineering of Polymers, Ministry of Education, Department of Macromolecular Science, Fudan University, Shanghai China

1. Introduction

Recently, silk fibroin has been widely attended for its biomedical material applications, because of its excellent properties such as strength, flexibility, biocompatibility and permeability (Altman et al., 2003). Compared with the silk fibroin from silkworm, spider fibroin has higher strength and stronger toughness, but its resource is limited. So people have tried to synthesize the spider fibroin using genetic recombination method to obtain the spider fibers (Fukushima, 1998; Heslot, 1998; Zhou et al., 2001). Shao et al. (Shao & Vollrath, 2002) demonstrated that although the amino acid sequence of *Bombyx mori* silkworm fibroin is different from that of spider fibroin, by controlling the process of the silkworm spinning, the high strength of the silk fiber as that of the spider fiber can be gained. The investigations indicate that there are the correlations among spinning process, secondary structure and mechanical properties of the silk fibroin. The environment of the silkworm spinning is changed during the process, such as shearing strength (Chen et al., 2001; Shao & Vollrath, 2002; Terry et al., 2004), pH (Magoshi et al., 1996; Xie et al., 2004; Zhou et al., 2004; Zong et al., 2004), concentration of metal ions (Li et al., 2001; Ruan et al., 2008; Zhou et al., 2004; Zong et al., 2004) and concentration of the silk fibroins (Magoshi et al., 1996; Terry et al., 2004), etc. Therefore, studying the environment effects on the silk fibroin conformation is benefit to understand the silkworm spinning mechanism, and helpful to synthesize artificially the silk fibroin or spidroin and fabricate the high performance silk fiber to meet the requirements of the biomaterial usages.

The methods used to investigate the silk fibroin mainly include X-ray diffraction (XRD) (Lv et al., 2005; March et al., 1955; Qiao et al., 2009; Takahashi et al., 1999; Saitoh et al., 2004; Sinsawat et al., 2002), electron diffraction (ED) (He et al., 1999), infrared (IR) (Chen et al., 2001; Mo et al., 2006), nuclear magnetic resonance (NMR) (Yao et al., 2004; Zhao et al., 2001) and so on. Among them, nuclear magnetic resonance spectroscopy is very effective to characterize the molecular chain structures of the biopolymers (Du et al., 2003; Li et al., 2008). Asakura et al. analyzed the crystal structures of 40 proteins and their NMR chemical shifts, and established the correlation of Ala, Ser, and Gly residues between ^{13}C chemical shifts of C_α, C_β atoms and the dihedral angels of φ and ψ of the peptide chains, which are very useful to determine the protein structure by NMR method (Asakura et al., 1999). The

authors also carried out a series of solid-state ^{13}C NMR experiments to study the peptides $(AG)_n$, a model compound of the silk fibroin, using spin diffusion NMR and rotational echo double resonance (REDOR) techniques (Asakura, 2001, 2002a, 2002b, 2002c, 2005a, 2005c, 2007). They found two types of the secondary structures of β-turn and β-sheet. The authors suggested that the peptides GAAS in the heavy chain of silk fibroin are one of the factors influencing the structural transition of the silk fibroin from random coil to β-sheet (Asakura et al., 2002) in which the –OH ligands of Ser residues participate in the formation of hydrogen bonds (Askura, 2002, 2005; Sato et al., 2008), and Tyr, replacing the Ser in the basic $(AGSGAG)_n$ sequence, can induce the partially disordered structure (Asakura et al., 2005). Ha et al. synthesized the non-crystalline silk peptide which contains 31 amino acid residues (GTGSSGFGPYVANGGYSGYEYAWSSESDFGT), and used high resolution 2D-NMR techniques, such as COSY, TOCSY, NOESY, ROESY and HMQC and HMBC, to study the structure of the peptide in solution. They proved that the structure of the peptide is a loop (Ha et al., 2005).

Our group has investigated the environmental influences on the conformation of silk fibroin by solid-state ^{13}C NMR during the past few years. Moreover, we also used EPR method to study the interaction between the metal ions of Cu^{2+}, Fe^{3+}, Mn^{2+} and silk fibroin, and tried to understand the role of the metal ions in the conformation transition. We are going to review our research results in this paper.

2. Component of silk fibroin and spinning process of the *Bombyx mori* silkworm

The heavy-chain fibroin is predominant component (up to 85% w/w) in *Bombyx mori* silk fibroin in addition to the light-chain fibroin including sericin and P25 (Couble et al., 1985; Tanaka et al., 1999). *Bombyx mori* silk fibroin (*B. mori* SF) has 5263 amino acid residues composed of 45.9% glycine (Gly), 30.3% alanine (Ala), 12.1% serine (Ser), 5.3% tyrosine (Tyr), 1.8% valine (Val), 0.25% tryptophan (Trp), 0.1% histidine (His) residues, etc. and has a molecular weight of 391 kDa (ExPASY, P05790, E.P.A.S.; P07856). Four types of repetitive sequence are mainly found in the heavy-chain silk fibroin, *i.e.* GAGAGS, GAGAGY and GAGAGVGY, forming hydrophobic domains, and eleven repetitive sequences GTGSSGFGPYVA(N/H)GGYSGYEYAWSSESDFGT forming fairly conserved hydrophilic spacers (Zhou et al., 2000). The silk fibroin exhibits excellent mechanical properties due to the primary structure of highly repetitive amino acid sequences $(GAGAGX)_n$, X = Ala, Ser, Tyr (Y), Val, etc., in which the repetitive hexapeptides $(GAGAGS)_n$ tend to be in the crystalline form, while $(GAGAGY)_n$ to be in the amorphous form to link the hydrophobic and hydrophilic domains along the protein chain (Mita et al., 1994; Shen et al., 1998).

During the natural silk spinning from the spinneret of a silkworm, the conformation of the silk fibroin is converted from a soluble helical form to an insoluble β-sheet form (Magoshi et al., 1996). Magoshi et al. (Kobayashi et al., 2001; Magoshi et al., 1996) found that pH changes gradually in the lumen of the silkworm from neutral (pH 6.9) in the posterior division to weakly acidic (pH 4.8) in the anterior division adjacent to the spinneret. Meantime, the concentration of the inorganic ions such as Ca^{2+}, K^+ and Mg^{2+} vary within each division of the silk gland (Hossain et al., 2003; Magoshi et al., 1996), which promotes the transition from gel to sol state and then formation of the silk fiber (Kobayashi et al., 2001).

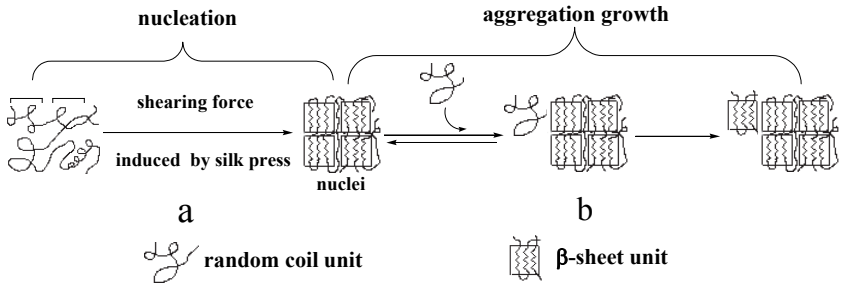

Fig. 1. Schematic illustration of the natural silk fibroin spinning process. (a) nucleation, which includes a transition of random coil to β-strand as well as a formation of the ordered β-sheet aggregates (nuclei); (b) aggregation growth, which involves the coiled chain changing its conformation on the preformed β-sheet nuclei, followed by formation of the larger β-sheet aggregation (From Li et al., 2001 with permission).

Li et al. (Li et al., 2001) used circular dichroism (CD) spectroscopy to study the conformation transition of the silk fibroin from random coil to β-sheet and the β-sheet aggregation growth. The authors suggested a nucleation-dependent aggregation mechanism for the silk spinning process as in Fig. 1. There are two steps involved in this mechanism: (a) nucleation, a rate-limited step involving the conversion of the soluble random coil to insoluble β-sheet and subsequently a series of thermodynamically unfavorable association of the β-sheet unit, *i.e.* the formation of a nucleus or seed; (b) once the nucleus forms, further growth of the β-sheet unit becomes thermodynamically favorable, resulting in a rapid extension of the β-sheet aggregation. The aggregation growth follows a first order kinetic process with respect to the fibroin concentration. The increase of the temperature accelerates the β-sheet aggregation growth if the β-sheet nucleus is introduced into the random coil fibroin solution. Meanwhile, the increase of the concentration of the metal ions, Ca^{2+}, K^{+}, Cu^{2+}, Zn^{2+} and Fe^{3+}, can also accelerate this change in some extent (Li et al., 2001; Ruan et al., 2008; L. Zhou et al, 2003; P. Zhou et al., 2004; Zong et al., 2004; Ji et al., 2009).
Moreover, the shearing strength plays a key role in the formation of fiber, and the cooperation with pH and metal ions is necessary in the spinning process. The natural evolution of the silkworm develops the special spinning process, leading to the excellent performance of the silk fiber. Therefore, understanding the silkworm spinning process is helpful for ones to manufacture the high performance artificial fibers.

3. Secondary structure of silk fibroin

There are mainly two typical conformations, Silk I and Silk II, in the crystalline/semi-crystalline domains of the heavy-chain silk fibroin. Kratky et al. (Kratky et al., 1950) found an unstable crystal domain approaching the spinneret, named "Silk I" which is dominated by the helix conformation, as well as another stable crystal domain in the spun fibers, named "Silk II" which is dominated by the β-sheet conformation. Valuzzi et al. (Valluzzi, 1996, 1997, 1999) found a 3_2-helical structure of *Bombyx mori* silk in ultrathin films formed at the air-water interface, named "silk III", indicating that the structure might be a transitional state from Silk I to Silk II. That means, in the spinning process, the Silk I conformation is transited to the Silk III conformation, and then to the Silk II conformation. There are many

NMR researches about Silk I and Silk II (Asakura, 1982, 1983, 1984; Kricheldorf et al., 1983; Saito, 1983, 1984; Zhou et al., 2001). The chemical shifts of the main amino acid residues, Gly and Ala, in *B. mori* silk fiber, degummed silk fiber and solid/liquid regenerated silk fibroin are listed in Table 1. The results show that different secondary structures have the different chemical shifts.

Samples	Conformation	Ala			Gly		Ref.
		C_α	C_β	C=O	C_α	C=O	
Cocoon	Silk II	49.7	20.2	171.7	43.9	169.4	Saito et al., 1983
Degummed silk	Silk II	48.6	20.2	172.2	43.1	169.6	Zhou et al., 2001
R. fibroin[a] (solid)	Silk II	49.7	20.0	172.5	43.0	172.5	Zhou et al., 2001
	Silk I	51.6	17.0	172.6	43.8	172.6	
R. fibroin (liquid)	Silk I	50.0	16.6	175.5	42.7	171.5	Asakura et al., 1984

Table 1. ^{13}C chemical shifts of *B. mori* silk and its regenerated fibroin (From Li et al., 2001 with permission). [a] regenerated fibroin.

Despite that the *B. mori* silk fibroin structures were extensively investigated by many experimental methods, *e.g.*, X-ray diffractions, molecular modelling calculations as well as solid-state ^{13}C NMR spectroscopy, a set of definitive structural parameters for both Silk I and Silk II forms are still unclear yet. We used a density functional theory (DFT) approach to assess those available structural parameters based on the comparison of calculated ^{13}C chemical shifts with experimental ones (Zhou et al., 2001). The results indicate that: (i) Silk I form (at 17.0 ± 0.5 ppm) is a 3_1-helixlike conformation with torsion angles of $<\varphi> = -59 \pm 2°$, $<\psi> = 119 \pm 2°$, $<\omega> = 178 \pm 2°$ for alanine residue and $<\varphi> = -78 \pm 2°$, $<\psi> = 149 \pm 2°$, $<\omega> = 178 \pm 2°$ for glycine residue in the silk fibroin; (ii) Silk II form (at 20.0 ± 0.5 ppm) individually determined by Marsh (Marsh et al., 1955), Fossey (Fossy et al., 1991) and Asakura (Asakura et al, 1985) are considered to be more rational than those determined by other authors. The resultant torsion angle are $<\varphi> = -143 \pm 6°$, $<\psi> = 142 \pm 5°$ and $<\omega> = 178 \pm 2°$ for both Ala and Gly residues. Besides, there are also transitional states: Silk I-like (at 15.0 ± 0.5 ppm) and Silk II-like (at 21.5 ± 0.5 ppm). Asakura studied the peptides $(AG)_n$ and indicated that the torsion angles of β-turn in Ala and Gly are (-62^o, 125^o) and (77^o, 10^o) (Asakura et al., 2005).

4. Environment influences on the transition of secondary structure of silk fibroin

The spinning process of the silkworm undergoes at normal temperature, normal pressure and aqueous solution with given shearing force, pH value, metallic ion contents and protein concentration.

Asakura et al. (Asakura et al., 1984) proved that the regenerated silk fibroin has the same amino acid sequence and secondary structure as the silk fibroin present in the silk gland. Therefore, we studied the solid regenerated silk fibroin which is prepared by dissolving the silk fiber in 9.3 M KBr solution and dialyzing and then drying in air in order to mimic the spinning process of water lost. The detail preparing process of the regenerated silk fibroin follows the reference report (Li et al., 2001).

4.1 Influence of pH

We used ^{13}C CP/MAS NMR spectroscopy to study the conformation of the silk fibroin within pH range of 5.2 - 8.0 (Xie et al., 2004). Fig. 2(A) shows ^{13}C CP/MAS NMR spectrum of the silk fibroin. The resonance peak at 5 ~ 25 ppm in Fig. 2(B) for the C_β of Ala residue can distinguish the helix form from the β-sheet form (Liivak et al., 1998). The lineshape of the peak can be deconvoluted into four components, Silk I at 17.0 ± 0.5 ppm and Silk II at 20.0 ±0.5 ppm, as well as transition state components, Silk I-like at 15.0 ± 0.5 ppm and Silk II-like at 21.5 ± 0.5 ppm (Zhou, 2004, 2001; Zong et al., 2004).

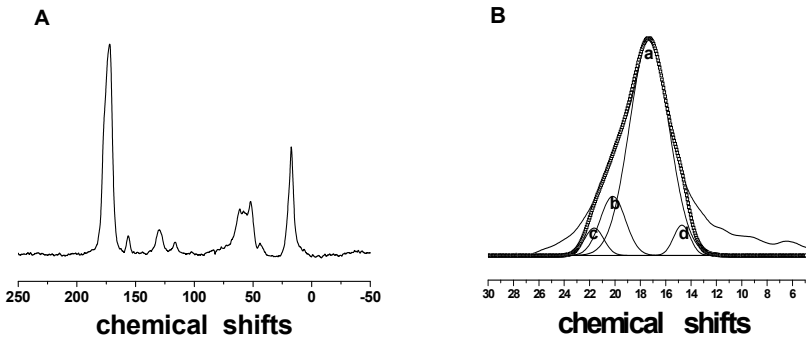

Fig. 2. (A) ^{13}C CP/MAS NMR spectrum of the regenerated silk fibroin. (B) Deconvolution result of the peak from 5 ~ 25 ppm resulting from the C_β of alanine. (a) Silk I (b) Silk II (c) Silk II-like (d) Silk I-like. The hollow squares are simulated spectra.

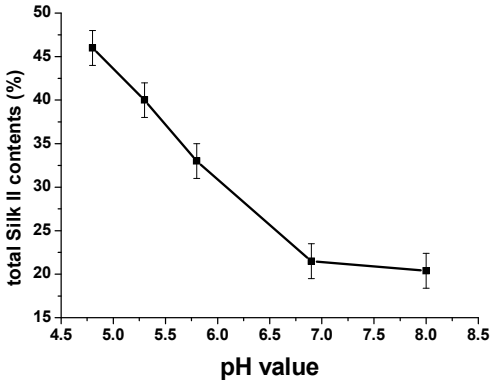

Fig. 3. The effect of pH values on total Silk II contents of silk fibroin.

We define the content of total Silk II conformation as the sum of Silk II and Silk II-like conformers, which is the conformation related to the β-sheet form. The dependence of total Silk II content on the pH change is shown in Fig. 3. It is found that as pH decreases, total Silk II content increases. It implies that a decrease in pH favors the conformation transition

from Silk I to Silk II. The reduction in negative charge by the protonation of the amino acids may promote a refolding to a more ordered state stabilized by the hydrogen bonding between chains and accompanied by an exclusion of water. The resulting orientation of the molecules and the reduction of the intermolecular distance could promote the formation of the Silk II conformation. Such a mechanism could account for the nucleation dependency of the aggregation and secondary structural transformation of the fibroin observed *in vitro* and postulated to occur *in vivo*.

4.2 Influence of Ca^{2+} and Cu^{2+}

Figure 4 demonstrates that the conformation conversion of the regenerated silk fibroin is dependent on the Ca^{2+} concentration (Zhou et al., 2004). The low pH (5.2) and the certain amount of Ca^{2+} ions (10 mg/g) favor the formation of Silk II and Silk II-related intermediate.

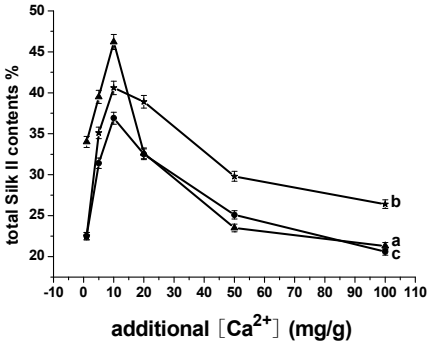

Fig. 4. Dependence of total Silk II conformations in silk fibroin at different [Ca^{2+}] and pH values. a, b, c represent the pH 5.2, 6.9, and 8.0, respectively (From Zhou et al., 2004 with permission).

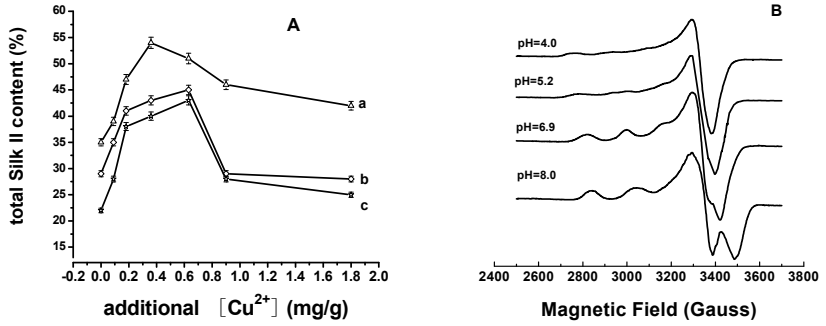

Fig. 5. (A) Dependence of total Silk II content at different added [Cu^{2+}] and pH values. a, b, c correspond to pH 5.2, 6.9, and 8.0, respectively; (B) EPR spectra of the Cu(II)/SF complexes at different pH values with added Cu(II) concentration of 1.80 mg/g (From Zong et al., 2004 with permission).

These results, although still lacking structural analysis in detail, may help to account for the role of pH and Ca^{2+} ions in the natural spinning process of the silkworms.

In addition, the high concentrations of Ca^{2+} ions partially inhibit the formation of Silk II-related conformation probably by introducing strong electrostatic interaction between molecular chains. It implies that, the relatively higher Ca^{2+} ion concentrations in the posterior division and the middle part of the middle division than that in the anterior part of the middle division in the silkworm gland (Terry et al., 2004) may prevent the premature β-sheet formation. The re-reduction of the Ca^{2+} ion content in the anterior division of the gland could be necessary to promote the gel to the sol transition for reducing the gel strength in native fibroin solutions and to permit it to flow through the spinning duct in the latter part of the secretory pathway (Hossain et al., 2003; Magoshi et al., 1994; Ochi et al., 2002).

In addition, we studied the Cu(II) ion influence on the silk fibroin conformation (Zong et al., 2004). From Fig. 5(A), we find that a small amount of Cu(II) addition leads to an increase in the content of total Silk II conformation and the content is highest when Cu(II) concentration is 0.36 mg/g at pH of 5.2, *i.e.*, the molar ratio of Cu to His residues in silk heavy chain is 0.76 : 1. Also, the content of total Silk II is highest when Cu(II) concentration is 0.63 mg/g at pH of 6.9 and 8.0, *i.e.*, the molar ratio of Cu to His residues is 1.33 : 1. However, further addition of Cu(II) (≧0.63 mg/g) results in a gradual reduction in the total Silk II conformation content, but there is still more total Silk II present in the silk fibroin samples with added Cu(II) than that in the samples without added Cu(II) (Fig. 5A).

Fig. 5(B) shows the EPR spectra of the Cu(II)/SF complex membranes prepared with the added Cu(II) concentration of 1.8 mg/g at pH 4.0, 5.2, 6.9, and 8.0, respectively. It is evident that the spectra are remarkably sensitive to pH variation. Table 2 summarizes the extracted parameters from the deconvoluted EPR traces, such as $g_{//}$, $g_{\perp}$, $A_{//}$, and $A_{\perp}$, and the deconvoluted components for the Cu(II)/SF complexes prepared with the added Cu(II) concentration of 1.8 mg/g at different pH values.

pH	Component	$A_{//}$[a]		$A_{\perp}$[a]		$g_{//}$[b]	$g_{\perp}$[b]	$g_{//}/A_{//}$	Relevant contents (%)[c]	Coordination modes
		G	$10^{-4}cm^{-1}$	G	$10^{-4}cm^{-1}$					
8.0		197	202	18	17	2.200	2.063	109	100	Cu~4N
6.9		182	190	16	15	2.235	2.068	117	100	Cu~3N1O
5.2	1	160	168	10	10	2.250	2.063	134	40	Cu~2N2O
	2	158	172	10	10	2.327	2.063	135	30	Cu~1N3O
	3	162	173	10	10	2.290	2.063	132	30	Cu~1N3O
4.0	1′	160	168	20	20	2.256	2.094	134	50	Cu~2N2O
	2′	164	177	20	20	2.317	2.094	131	50	Cu~1N3O

Table 2. Summary of EPR parameters and coordination modes for the Cu(II)/SF complexes prepared at different pH values with the added Cu(II) concentration of 1.8 mg/g (From Zong et al., 2004 with permission). [a] A (cm^{-1}) = $0.46686 \times 10^{-4} \times g \times A$ (Gauss), and the absolute error in all reported A values is less than ± 2 G. [b] Absolute error in g-values ± 0.002. [c] Relevant error in all reported contents is less than 2%.

The simulated results of the EPR spectra of the Cu(II)/SF complexes at pH 8.0 and 6.9 indicate that the Cu(II) coordination with silk fibroin forms predominantly a square-planar complex with coordination modes of Cu-4N (one Cu atom coordinates four nitrogen atoms) at pH of 8.0 and Cu-3N1O (one Cu atom coordinates three nitrogen atoms and one oxygen atom) at pH of 6.9. As we know, the number of deprotonated nitrogen atoms will increase at higher pH, resulting in more possibilities for Cu(II) coordination to the nitrogen atoms.

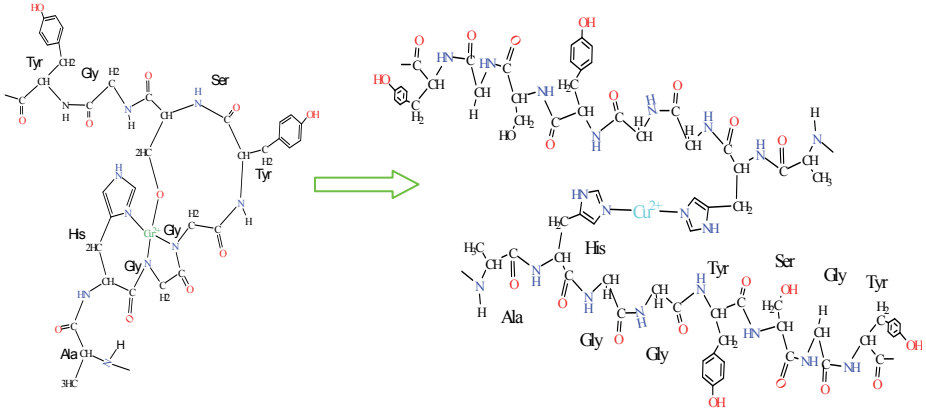

Under neutral and basic condition Under weakly acidic condition

A B

Fig. 6. Models for the Cu(II)/SF complex at neutral (A) and weakly acidic conditions (B) (From Zong et al., 2004 with permission).

In the amorphous domain of *B. mori* silk fibroin chain, which links two crystalline domains, there exist three conserved AHGGYSGY peptides in a silk fibroin heavy chain (Zhou et al., 2000), similar to the peptide sequence of PHGGGWGY in PrP (Donne et al., 1997; Riek et al., 1997). The pH-dependent Cu(II) EPR and coordination modes in the Cu(II)/PrP (Aronoff-Spencer et al., 2000; Miura et al., 1999) and Cu(II)/Aβ (Miura et al., 2000) complexes are strikingly similar to that of the Cu(II)/SF complexes observed here. Therefore, we suggest that the coordination modes and binding sites of Cu(II) with the silk fibroin are similar to those in PrP protein. At neutral pH, Cu(II) coordinates with silk fibroin as a mode of Cu-3N1O. The peptides AHGGYSGY in the silk fibroin may form a complex with Cu(II) by coordination *via* the imidazole N_{π} atom of the His side chain together with two deprotonated main-chain amide nitrogens in the two glycine residues and one hydroxyl in the serine residue (Fig. 6(A)). Under weakly acidic conditions (pH 5.2 - 4.0), the Cu(II) coordination mode may change to Cu-2N2O (one Cu atom coordinates two nitrogen atoms and two oxygen atoms), where Cu (II)-binding site with His residue changes from N_{π} to N_{τ} to share a Cu(II) ion between two His residues in the different peptide chains (Fig. 6(B)). The coordination mode of Cu-1N3O (one Cu atom coordinates one nitrogen atom and three oxygen atoms) may stem from Cu(II) binding one N_{τ} of the His residue and three oxygen atoms from the carbonyl of glycine and serine residues or from water (Aronoff-Spencer et al., 2000).

4.3 Influence of K^+ of Na^+

K^+ ion influence on the silk fibroin conformation was investigated by ^{13}C NMR and Raman Spectroscopy (Ruan et al., 2008). Fig. 7(A) shows that, as the added [K^+] increases from 0 to 3.7 mg/g, the silk fibroin conformations change partially from helix to β-sheet (Ruan et al., 2008). However, further increase of [K^+] from 3.7 to 12.5 mg/g induces a decrease in total Silk II content. In addition, Fig. 7(B) shows that, as [K^+] increases from 0 to 3.7 mg/g, the chemical shift of the tyrosyl C_α apical peak moves from the lower field (57.5 ± 0.5 ppm) to the higher field (55.5 ± 0.5 ppm). The change in the tyrosyl C_α chemical shift is thought changing in the environment of the tyrosine within the repetitive crystalline blocks as the fibroin conformation changes from Silk I to Silk II (Asakura et al., 2002; Taddei et al., 2004). It confirms the earlier evidence (Asakura et al., 2002; Taddei et al., 2004) that the environment of the tyrosine residues in the fibroin undergoes a change in hydrophobicity during the formation of β-sheets.

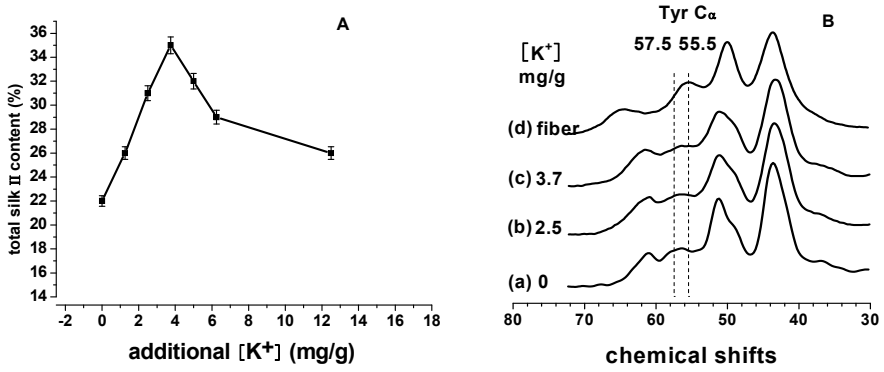

Fig. 7. Effect of [K^+] on the silk fibroin conformation. (A) effect of the added [K^+] on the total Silk II conformations. (B) solid-state ^{13}C CP/MAS NMR spectra of the tyrosine residues of silk fibroin with added [K^+] at (a) 0, (b) 2.5, (c) 3.7 mg/g, and that of silk fiber (d) (From Ruan et al., 2008 with permission).

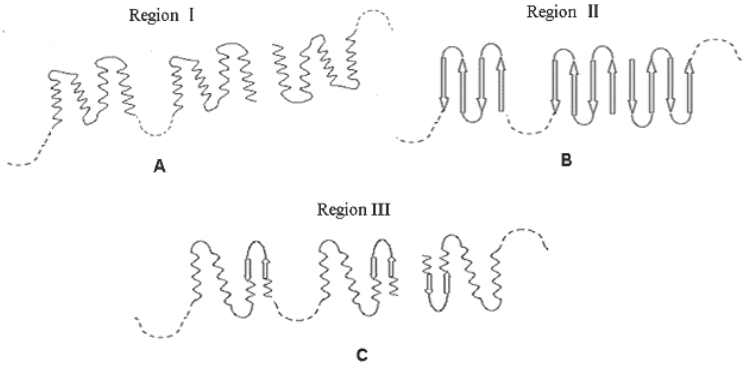

Fig. 8. Schematic representation of the hypothetical changes in heavy-chain fibroin structure induced by a progressive increase in [K^+] (From Ruan et al., 2008 with permission).

The sequence of *Bombyx mori* heavy-chain silk fibroin has a large number of the palindrome sequences of VGYG (21 repeats)/GYGV (11 repeats), and those special sequences oppose one another at the ends of the extended β-stands (Zhou et al., 2000). At a high K^+ ion concentration in the fibroin, these ions may interact with carbonyl oxygen atoms from VGYG/GYGV palindrome sequences.

Combining the NMR and Raman results focused on the tyrosine change (Ruan et al., 2008), we propose a process of molecular chain movement shown in Fig. 8 as [K^+] is increased. In region I of Fig. 8, as the added [K^+] increases from 0 to 1.2 mg/g, the tyrosine changes from a hydrophobic environment to the environment in which there is moderate hydrogen bonding. We suggest that, when the regenerated silk fibroin is in the helix (Silk I) and/or random coil conformation, the tyrosyl groups exist in a highly hydrophobic environment. The packing of the helix structure with an intra-chain H-bond is unfavorable for the phenolic-OH hydrogen-bonding interactions (Taddi et al., 2004). An increase in [K^+] may induce movement of the main chains, causing tyrosine to leave its hydrophobic environment and be exposed on the surface of protein when the fibroin is in the helix-like conformation. This change in the tyrosine environment may allow the phenolic-OH oxygen to act as an acceptor of a hydrogen atom as the serine hydroxyl group to do in the silk fibroin main chain (Taddei et al., 2004) with weakly hydrogen-bonding strength, causing the silk fibroin to undergo a secondary structural transition to the Silk II conformation. As the added [K^+] increases from 1.2 to 3.7 mg/g (region II), the phenolic-OH acts progressively as an acceptor of strong hydrogen bonding, giving rise to the β-sheet-related conformation. At a [K^+] of 3.7 mg/g, the hydrogen bonding between tyrosine phenolic-OH oxygen and the main chain hydrogen donor in the β-sheet conformation is strongest at the point at which the total Silk II content reaches its maximum. However, a further increase in the [K^+] up to 6.2 mg/g may result in some decrease in β-sheet-like conformation and the disordered intermediate re-appears. As added [K^+] increases from 6.2 to 12.5 mg/g (region III), the silk fibroin conformation is thought to return to the helix and/or random coil state. This may result from the tendency of the ions to prevent β-sheet hydrogen bond formation at high fibroin concentrations as a consequence of its chaotropic effect. In region III, the tyrosine residues have returned to a hydrophobic environment.

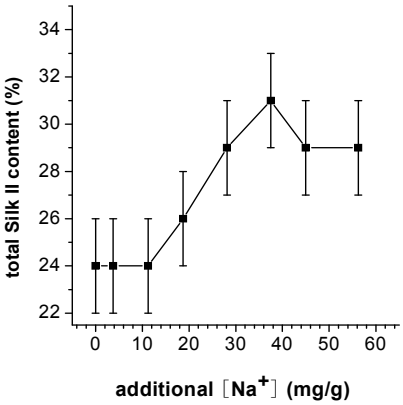

Fig. 9. Dependence of total Silk II contents upon [Na^+] (From Ruan & Zhou, 2008 with permission).

Moreover, we investigated Na^+ ion effect on the silk fibroin conformation (Ruan et al., 2008). Samples are Na^+-contained regenerated silk fibroin films. ^{13}C CP/MAS NMR demonstrates that as the added [Na^+] increases, partial silk fibroin conformation transit from helix-form to β-form at certain Na^+ ion concentration which is much higher than that in *B. mori* silkworm gland. Fig. 9 shows the dependence of total Silk II content upon [Na^+]. As [Na^+] increase from 0 to 11.2 mg/g, there is no significant change in the Silk II content, and as [Na^+] increase up to 37.5 mg/g, the Silk II content increases from original 24% to the highest of 31%. As [Na^+] further increase to 56.2 mg/g, the Silk II content slightly drops down from 31% to 29%. The influence of Na^+ ion on the silk fibroin conformation is not so evident as that of Ca^{2+}, Cu^{2+} and K^+ ions.

4.4 Influence of ferric and ferrous ions

Fe^{3+}/SF and Fe^{2+}/SF samples were studied with ^{13}C CP/MAS NMR spectroscopy to compare the different effects of ferric and ferrous ions on the conformation of silk fibroin. The effect of ferric and ferrous ions on the Silk II contents is shown in Fig. 10 (Ji et al., 2009). Within the range 0 - 75.0 μg/g of iron ions contents, Silk II contents for Fe^{3+}/SF and Fe^{2+}/SF are closely comparable: slowly decreasing but lying between 17% and 22%. However, when iron ions exceed 75 μg/g, Silk II content of Fe^{3+}/SF samples increased progressively and markedly up to about 40% at 125 μg/g of [iron] (Fig. 10-a), but that of Fe^{2+}/SF samples only increased slightly (Fig. 10-b). It indicated that a small amount of ferric ions could maintain the ratio of [helix-form]/[β-sheet form] as constant in the silk fibroin. But if more ferric ions were added, more β-sheet structures would be formed due to the interaction of ferric ions with the specific residues in fairly conserved hydrophilic spacers in the heavy chain fibroin sequence. Once the folding template was formed, the folding process would be markedly accelerated (Gillmor et al., 1997) because of the strong hydrophobic interactions between the hydrophobic spacers in the silk fibroin, leading to the aggregation of β-sheet components. The process was demonstrated nucleation dependent (Li et al., 2001).

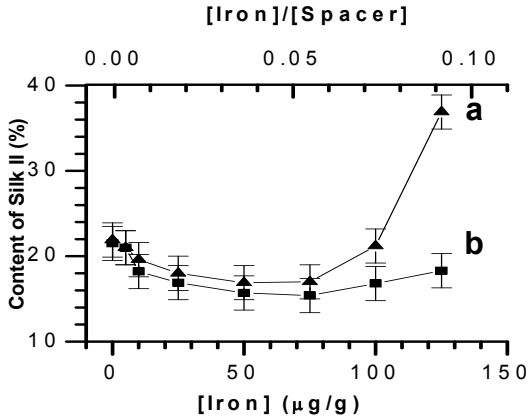

Fig. 10. Dependence of Silk II contents (including β-sheet and β-sheet-like components) on the added [Fe^{3+}] or [Fe^{2+}] in silk fibroin: (a) Fe^{3+}/SF samples, (b) Fe^{2+}/SF samples. The simulation error is ± 2% (From Ji et al., 2009).

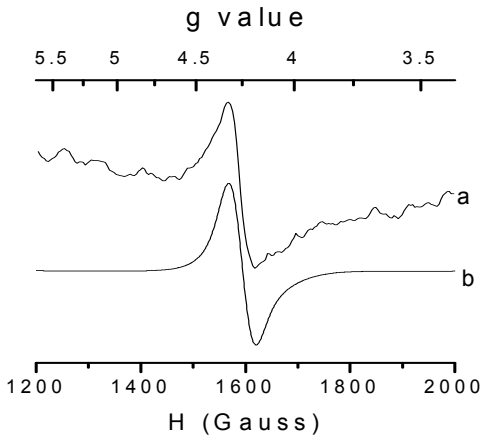

Fig. 11. The experimental (a) and simulated (b) EPR spectra of Fe^{3+}/SF sample with the added [Fe^{3+}] of 75.0 μg/g under the magnetic field strength of 9.45 GHz, T = 100 K. The simulated parameters are as follows: g_1 = 1.950, g_2 = 1.990, g_3 = 1.995, D = 2 cm^{-1} and E/D = 1/3 and the line width peak to peak is 4 MHz (From Ji et al., 2009 with permission).

Fe^{3+}/SF samples with [Fe^{3+}] of 75.0 and 125.0 μg/g were measured by EPR spectrometer. Fe^{3+}/SF sample with [Fe^{3+}] of 75.0 μg/g has the lowest Silk II content while that with [Fe^{3+}] of 125.0 μg/g has the highest Silk II content (see Fig. 10), but they have a similar EPR spectrum as shown in Fig. 11-a with [Fe^{3+}] of 75.0 μg/g. Only one signal at $g' \sim 4.25$ was observed, which implied that the transition occurred at energy level 3 → 4 (Bou-Abdallah & Chasteen, 2008). The EPR signal of pure $FeCl_3$ sample was not observed in the samples. Fig. 11-b is the simulated spectrum. The parameters extracted from the simulation are as follows: the zero-field-splitting interaction D = 1.2 ~ 2 cm^{-1} which is larger than the applied magnetic field B of 0.315 cm^{-1} (i.e. X-band) in our experiment; E/D = 1/3; the theoretic g-value = 1.950, 1.990, and 1.995. Based on the apparent g-value, g' = 4.25, and those simulated parameters, we could conclude that the ferric ions in the silk fibroin are at high-spin state of S = 5/2 and low symmetric site (Teschner et al., 2004).

Bou-Abdallah and Chasteen (Bou-Abdallah & Chasteen, 2008) assigned the EPR signal of g' = 4.25 with zero-field-splitting interaction of $|D| \leq 2$ cm^{-1} and E/D = 1/3, to a mononuclear high-spin ferric ions (S = 5/2) in a site of low symmetry, which is often observed in many proteins (Aasa et al., 1963; Solomon et al., 2000; Taboy et al., 2001). Tyrosine, histidine, glutamine and aspartate generally have a strong ability to coordinate with ferric ions. All of those residues are located in the spacer regions of the proteins. Interestingly, the 11 highly conserved hydrophilic spacers TGSSGFGPYVAN(H)GGYSGYEYAWSSESDFGT in the heavy chain of silk fibroin also play a role as a linker and include all of the residues which are considered as potential binding sites for the ferric ions. The spacer in silk fibroin connects two regularly arranged sequences, i.e. $(GAGAGS)_n$ and/or $(GA(V)GAGY)_n$ in helix-form (Silk I) or β-sheet form (Silk II). As a result, silk fibroin might bind to ferric ions with those residues in the hydrophilic spacers. If ferric ions were trapped in such regions, the β-sheet folding center might be formed, and thereafter the folding process could be accelerated if more ferric ions were added.

4.5 Influence of Mn^{2+}

Figure 12 shows the EPR spectra of Mn(II)/SF samples which were prepared from samples with an initial pH's of 7.5, 6.0 and 5.2 (Deng et al., 2011). All three spectra shown in Figure 12-c's with the added Mn(II) contents of 40.0 μg/g were almost identical, indicating that the environments of the Mn(II) ions were not pH dependent. Fig. 12-d's show typical sextet splitting along with double peaks between the adjacent peaks, very similar to that of $MnCl_2$ in 12 M HCl aqueous solution and in methyl alcohol solution at frozen state (T = 90 K) (Allen & Nebert, 1964), where Mn^{2+} ion is in the $Mn(H_2O)_6^{2+}$ complex. However, Figure 12-a's and 12-b's with Mn(II) contents of 4.0 and 10.0 μg/g, respectively, show somewhat pH dependency; the sextet splitting becomes evident as pH decrease from 7.5 to 5.2.

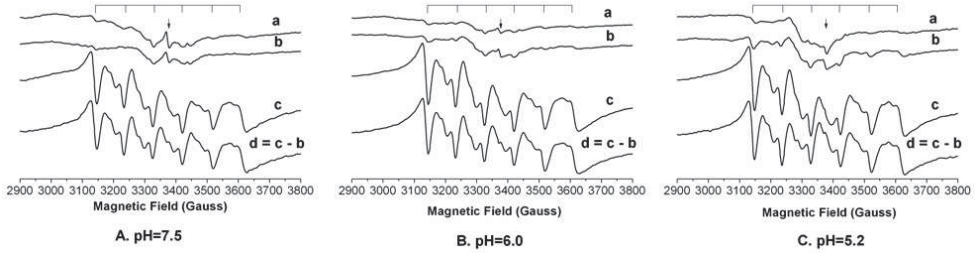

Fig. 12. Dependence of EPR spectra of [Mn(II)]/SF samples with different added contents of Mn(II) upon pH. (a), (b), (c) represent the added [Mn(II)] of 4.0, 10.0, 40.0 μg/g under pH of 7.5 (A), 6.0 (B), 5.2 (C), respectively. The peaks marked with arrows are free radical signals, respectively. The six stick-lines on the top of figure indicate the sextet splitting of Mn(II) with A = 96 G. All the spectra were recorded at 100 K, υ = 9.45 GHz, sweep width = 1500 G (From Deng et al., 2011 with permission).

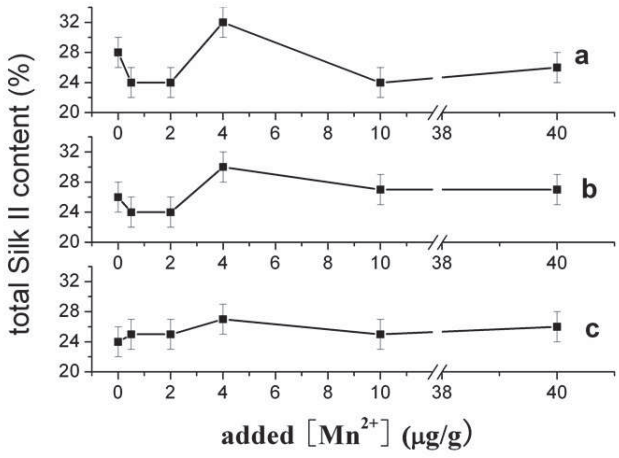

Fig. 13. Dependence of total Silk II (summary of Silk II and Silk II-like) conformations on the added [Mn(II)] at pH of 7.5 (a), 6.0 (b), and 5.2 (c) (From Deng et al., 2011 with permission).

^{13}C CP/MAS NMR of silk fibroin was studied to investigate the effect of Mn(II) ions on the conformational transition of silk fibroin. Fig. 13 (Deng et al., 2011) shows the dependence of total Silk II contents (including Silk II and Silk II-like conformations) upon the added Mn(II) content and pH. Mn(II) ions over the concentration range studied show no detectable effect on the Silk II content except for a very small but significant increase by 5% in Silk II conformation at Mn(II) content of 4.0 μg/g and pH from 5.2 to 7.5. The total Silk II maximum content of 32 ± 2% was observed at the added [Mn(II)] of 4.0 μg/g and at pH of 7.5, while the content is much lower compared with the content of 54 ± 2% obtained by adding cupric ions to the regenerated SF (Zong et al., 2004). Besides, the EDTA-treated silk fibroin had almost the same NMR spectrum as pure silk fibroin (data not shown). These observations indicate that Mn(II) had no detectable effect on the promotion of the conformation transition in SF. Those results indicate that there are two types of Mn(II) complexes present in the silk fibroin: one is six-coordinated Mn(II)/SF complex when the content of Mn(II) is small (less than 10.0 μg/g), and the other is $Mn(H_2O)_6^{2+}$ complex which predominates at higher Mn(II) concentrations. The six-coordinated complex may be formed with the Asp, Glu and His residues in the hydrophilic spacers, promoting the Silk II conformation. In contrast, the $Mn(H_2O)_6^{2+}$ complex might stabilize the first water shell thereby tending to maintain the silk fibroin Silk I conformation, therefore leading to the pH almost hardly influencing the conformation transition of the silk fibroin. Mn(II) ions, existing in the silk gland (Zhou et al., 2005), may play a role in maintaining the appropriate balance of the secondary structure components including helix-form and β-form to keep the silk fibroin stable in liquid state in the secretory pathway.

Dependence of the silk fibroin secondary structure transition upon different added metal ions is summarized in Table 3. From Table 3, Ca^{2+}, Cu^{2+}, K^+, Fe^{3+} ions show the evident effect on the conformation transition of the silk fibroin, while Na^+, Fe^{2+} and Mn^{2+} ions show a weak effect.

Metal Ions	Silk I to Silk II transition	references
Ca^{2+}	yes	Zhou et al., 2004
Cu^{2+}		Zong et al., 2004
K^+		Ruan et al., 2008
Fe^{3+}		Ji et al., 2009
Na^+	no	Ruan et al., 2008
Fe^{2+}		Ji et al., 2009
Mn^{2+}		Deng et al., 2011

Table 3. Dependences of the silk fibroin secondary structure transition upon different added metal ion.

5. Conclusion

The function of protein is closely dependent on the structure of protein. The components and the secondary structures of the silk fibroin evidently affect the mechanical properties of the structural protein. Magnetic resonance methods (NMR and EPR) demonstrate that the conformation of the silk fibroin can be changed from random coil and/or helix to β-sheet under certain pH value and metal ion concentration along with the change in the coordination of silk fibroin with the metal ions as well as the change in the hydrophilic and hydrophobic environments of the protein. The results are helpful for understanding the

mechanism of silkworm spinning and will give the guidance for fabricating the artificially high performance biomaterials.

6. Acknowledgements

The projects were supported by National Natural Science Foundation of China (Nos. 10475017, 20434010, 20673022 and 29974004). We also thank many dedicated coworkers who have contributed to the researches.

7. References

Aasa R, Malmstroem BG & Saltman P, *Biochim Biophys Acta* 75:203 (1963).
Altman GH, Diaz F, Jakuba C, *et al, Biomaterials* 24:401 (2003).
Aronoff-Spencer E, Burns CS, Avdievich NI, *et al, Biochemistry* 39:13760 (2000).
Asakura T & Ando M, *Makromol Chem Rapid Commun* 3:723 (1982).
Asakura T, Suzuki H & Watanabe Y, *Macromolecules* 16:1024 (1983).
Asakura T, Watanabe Y, Uchida A, *et al, Macromolecules* 17:1075 (1984).
Asakura T, Kuzuhara A, Tabeta R & Saito H, *Macromolecules* 18:1841 (1985).
Asakura T, Iwadate M, Demura M, *et al, Int J Biol Macromol* 24:167 (1999).
Asakura T, Ashida J, Yamane T, *et al, J Mol Biol* 306:291 (2001).
Asakura T & Yao JM, *Protein Sci* 11:2706 (2002).
Asakura T, Sugino R & Yao JM, *Biochemistry* 41:4415 (2002).
Asakura T, Sugino R, Okumura T, *et al, Protein Sci* 11:1873 (2002).
Asakura T, Yao JM, Yamane T, *et al, J Am Chem Soc* 124:8794 (2002).
Asakura T, Ohgo K, Ishida T, *et al, Biomacromolecules* 6:468 (2005).
Asakura T, Ohgo K, Komatsu K, et al, *Macromolecules* 38:7397 (2005).
Asakura T, Nakazawa Y, Ohnishi E, *et al, Protein Sci* 14:2654 (2005).
Asakura T, Sato H, Moro F, et al, *J Am Chem Soc* 129:5703 (2007).
Bou-Abdallah F & Dennis Chasteen N, *J Biol Inorg Chem* 13:15 (2008).
Chen X, Knight DP, Shao ZZ & Vollrath F, *Polymer* 42:9969 (2001).
Chen X, Shao ZZ, Marinkovic NS, *et al, Biophys Chem* 89:25 (2001).
Couble P, Chevillard M, Monie A, Ravel-Chapuis P & Prudhomme JC, *Nucleic Acids Res* 13:1801 (1985).
Deng YB, Ji D, Sun PC, *et al, Spectrosc Lett* 44:176 (2011).
Donne DG, Viles JH, Gorth D, Mehlhorn I, James TL, Cohen FE, Prusiner SB, Wright PE & Dyson HJ, *Proc. Natl. Acad. Sci.USA* 94:13452 (1997).
Du DZ, Wu DC & Pan CY, *Chinese J Magn Reson* 20:363 (2003).
ExPASy, P05790, E. P. A. S.; P07856.
Fossy SA, Nemethy G, Gibson KD & Scheraga HA, *Biopolymer* 31:1529 (1991).
Fukushima Y, *Biopolymers* 45:269 (1998).
Gillmor SA, Villasenor A, Fletterick R, *et al, Nat Struct Biol* 4:1003 (1997).
Ha SW, Gracz HS, Tonelli AE, *et al, Biomacromolecules* 6:2563 (2005).
He SJ, Valluzzi R & Gido SP, *Int J Biol Macromo* l24:187 (1999).
Heslot H, *Biochimie* 80:19 (1998).
Hossain KS, Ochi A, Ooyama E, *et al, Biomacromolecules* 4:350 (2003).
Ji D, Deng YB and Ping Z, *et al, J Mol Struct* 938:305 (2009).
Kobayashi M, Tanaka T, Inoue SI, Tsuda H, Magoshi J, Magoshi Y & Becker MA, *Polymer prepr* 42:294 (2001).
Kratky O, Schauenstein E & Sekora A, *Nature* 165:319 (1950).

Kricheldorf HR, Muller D & Ziegler K, *Polym Bull* 9:284 (1983).
Liivak O, Blye A, Shah N, *et al, Macromolecules* 31:2947 (1998).
Li GY, Zhou P, Shao ZZ, *et al, Eur J Biochem* 268:6600 (2001).
Li GY, Zhou P, Sun YJ, *et al, Chem J Chin Univ* 22:860 (2001).
Li J, Xu FL, Xie, MR, et al, *Chinese J Magn Reson* 25:11 (2008).
Lv Q, Cao CB & Zhu HS, *Polymer Int* 54:1076 (2005).
Miura T, Hori-I A, Mototani H, *et al, Biochemistry* 38:11560 (1999).
Miura T, Suzuki K, Kohata N, *et al, Biochemistry* 39:7024 (2000).
Magoshi J, Magoshi Y & Nakamura S, *Silk Polymers-Materials Science and Biotechnology* 544:292 (1994).
Magoshi J, Magoshi Y, Becker MA & Nakamura S, *In Polymeric Materials Encyclopedia (Salamone JC, ed.), vo*l. 1: Biospinning (silk fiber formation, multiple spinning mechanisms). CRC Press: New York (1996).
Marsh RE, Corey RB & Pauling L, *Biochim Biophys Acta* 16:1 (1955).
Mita K, Ichimura S & James T, *J. Mol. Evol* 38:583 (1994).
Mo CL, Wu PY, Chen X, *et al, Appl Spectrosc* 60:1438 (2006).
Ochi A, Hossain KS, Magoshi J & Nemoto N, *Biomacromolecules* 3:1187 (2002).
Qiao XY, Li W, Sun K, Xu S & Chen XD, *Polymer Int* 58:530 (2009).
Riek R, Hornemann S, Wider G, Glockshuber R & Wuthrich K, *FEBS Lett* 413:282 (1997).
Ruan QX & Zhou P, *J Mol Struct* 883:85 (2008).
Ruan QX, Zhou, P, Hu, BW, *et al, FEBS J* 275:219 (2008).
Sinsawat A, Putthanarat S, Magoshi Y, *et al, Polymer* 43:1323, (2002).
Saito H, Iwanaga Y, Tabeta R, *et al, Chem Lett* 12:427 (1983).
Saito H, Tabeta R, Asakura T, *et al, Macromolecules* 17:1405 (1984).
Saito H, Ohshima K, Tsubouchi K, *et al, Int J Biol Macromol* 34:317 (2004).
Sato H, Kizuka M, Nakazawa Y, *et al, Polym J* 40:184 (2008).
Shao ZZ & Vollrath F, *Nature* 418:741 (2002).
Shen Y, Johnson MA & Martin DC, *Macromolecules* 31:8857 (1998).
Solomon EI, Brunold TC, *et al, Chem Rev* 100:235 (2000).
Taboy CH, Vaughan KG, Mietzner TA, *et al, J Biol Chem* 276:2719 (2001).
Taddei p, Asakura T, Yao JM & Monti P, *Biopolymers* 75:314 (2004).
Takahashi Y, Gehoh M & Yuzuriha K, *Int J Biol Macromol* 24:127 (1999).
Tanaka K, Inoue S & Mizuno S, *Insect biochem Mol Biol* 29:269 (1999).
Terry AE, Knight DP, Porter D & Vollrath F, *Biomacromolecules* 5:768 (2004).
Teschner T, Trautwein AX, Schunemane V, *et al, Hyperfine Interact* 156/157:285 (2004).
Valluzzi R, Gido SP, Zhang WP, *et al, Macromolecules* 29:8606 (1996).
Valluzzi R & Gido SP, *Biopolymers* 42:705 (1997).
Valluzzi R, Gido SP, Muller W & Kaplan DL, *International Journal of Biological Macromolecules* 24:237 (1999).
Xie X, Zhou P, Deng F, *et al, Chem J Chinese Universities* 25:961 (2004).
Yao J M, Nakazawa Y & Asakura T, *Biomacromolecules* 5:680 (2004).
Zhao C & Asakura T, *Prog Nucl Magn Reson Spectrosc* 39:301 (2001).
Zhou CZ, Confalonieri F, Medina N, *et al, Nucleic Acids Res* 28:2413 (2000).
Zhou L, Chen X, Shao ZZ, *et al, FEBS Lett* 554:337 (2003).
Zhou L, Terry AE, Huang YF, *et al, Acta Chim Sinica* 63:1379 (2005).
Zhou P, Li GY, Shao ZZ, *et al, J Phys Chem B* 105:12469 (2001).
Zhou P, Xie X, Deng F, *et al, Biochemistry* 43:11302 (2004).
Zhou Y, Wu S & Conticello VP, *Biomacromolecules* 2:111 (2001).
Zong XH, Zhou P, Shao, ZZ, *et al, Biochemistry* 43:11932 (2004).

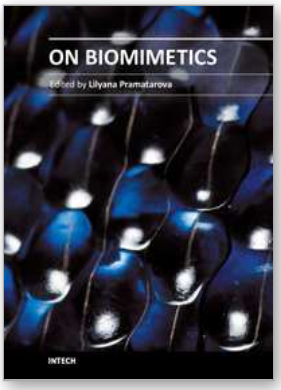

On Biomimetics

Edited by Dr. Lilyana Pramatarova

ISBN 978-953-307-271-5
Hard cover, 642 pages
Publisher InTech
Published online 29, August, 2011
Published in print edition August, 2011

Bio-mimicry is fundamental idea â€˜How to mimic the Natureâ€™ by various methodologies as well as new ideas or suggestions on the creation of novel materials and functions. This book comprises seven sections on various perspectives of bio-mimicry in our life; Section 1 gives an overview of modeling of biomimetic materials; Section 2 presents a processing and design of biomaterials; Section 3 presents various aspects of design and application of biomimetic polymers and composites are discussed; Section 4 presents a general characterization of biomaterials; Section 5 proposes new examples for biomimetic systems; Section 6 summarizes chapters, concerning cells behavior through mimicry; Section 7 presents various applications of biomimetic materials are presented. Aimed at physicists, chemists and biologists interested in biomineralization, biochemistry, kinetics, solution chemistry. This book is also relevant to engineers and doctors interested in research and construction of biomimetic systems.

InTech Europe
University Campus STeP Ri
Slavka Krautzeka 83/A
51000 Rijeka, Croatia
Phone: +385 (51) 770 447
Fax: +385 (51) 686 166
www.intechopen.com

InTech China
Unit 405, Office Block, Hotel Equatorial Shanghai
No.65, Yan An Road (West), Shanghai, 200040, China
中国上海市延安西路65号上海国际贵都大饭店办公楼405单元
Phone: +86-21-62489820
Fax: +86-21-62489821